MITSUBISHI ELECTRIC RESEARCH LABORATORIES
http://www.merl.com

# Targeted Energy Transfer for Suppressing Regenerative Instabilities in a 2-DOF Machine Tool Model

Nankali, A.; Kalmar-Nagy, T.; Lee, Y.S.

TR2013-072 August 2013

**Abstract**

We study targeted energy transfer (TET) mechanisms by applying a nonlinear energy sink (NES) to suppress regenerative instabilities in a 2-DOF planar machine tool model. With the help of a numerical continuation tool, DDEBIFTOOL, we show that the tool instability is generated through a subcritical Hopf bifurcation in this simplified tool model. Studying modal energy exchanges reveals that only one of the DOFs is predominant, which may lead to the standard single-DOF machine tool model. Then, we apply an ungrounded NES to the 2-DOF tool model such that the NES interacts only with the dominant mode, which turns out to be more efficient than applying the NES to the other insignificant mode. Simple numerical simulations and bifurcation analysis demonstrate that the three typical TET mechanisms can be identified - That is, recurrent burst outs and suppression, and partial and complete suppression of tool instability.

*ASME International Design Engineering Technical Conferences & Computers and Information in Engineering Conference (IDETC/CIE)*

# TARGETED ENERGY TRANSFER FOR SUPPRESSING REGENERATIVE INSTABILITIES IN A 2-DOF MACHINE TOOL MODEL

**Amir Nankali**
Department of Mechanical Engineering
University of Michigan, Ann-Arbor

**Young S. Lee**
Department of Mechanical and Aerospace Engineering
New Mexico State University
Las Cruces, NM 88003, USA

**Tamas Kalmar-Nagy**
Mitsubishi Electric Research Laboratories
201 Broadway, Cambridge, MA 02139, USA

## ABSTRACT

*We study targeted energy transfer (TET) mechanisms by applying a nonlinear energy sink (NES) to suppress regenerative instabilities in a 2-DOF planar machine tool model. With the help of a numerical continuation tool, DDEBIFTOOL, we show that the tool instability is generated through a subcritical Hopf bifurcation in this simplified tool model. Studying modal energy exchanges reveals that only one of the DOFs is predominant, which may lead to the standard single-DOF machine tool model. Then, we apply an ungrounded NES to the 2-DOF tool model such that the NES interacts only with the dominant mode, which turns out to be more efficient than applying the NES to the other insignificant mode. Simple numerical simulations and bifurcation analysis demonstrate that the three typical TET mechanisms can be identified - That is, recurrent burstouts and suppression, and partial and complete suppression of tool instability.*

## INTRODUCTION

Regenerative effects in machining arises from the fact that the cutting force exerted on a tool is influenced not only by the current position but also by that in the previous revolution. Hence, the equation of motion for the tool appears as a delay differential equation, which renders even an SDOF dynamical system to be infinite-dimensional (See, for example, Dombovari et al. [1] and Nayfeh and Nayfeh [2] for recent studies on machine tool dynamics).

In practical machining process, regenerative LCOs would create adverse effects on machining quality, and various passive and active means have been considered to improve machining stability boundary (e.g., see [3–8]). In particular, direct use or variations of linear/nonlinear tuned mass damper (TMD [7, 8]) are probably the most popular approach to passive chatter suppression. However, even if the TMD is initially designed (tuned) to eliminate resonant responses near the eigenfrequency of a primary system, the mitigating performance may become less effective over time due to aging of the system, temperature or humidity variations and so forth, thus requiring additional adjustment or tuning of parameters.

It is only recently that passively controlled spatial (hence dynamic) transfers of vibrational energy in coupled oscillators to a targeted point where the energy eventually localizes were studied by utilizing an NES (See Vakakis et al. [9] for the summary of up-to-date developments); and this phenomenon is simply called targeted energy transfer (TET). The NES is basically a device that interacts with a primary structure over broad frequency bands; indeed, since the NES possesses essential stiffness non-linearity, it may engage in (transient) resonance capture [10] with any mode of the primary system. It follows that an NES can be designed to extract broadband vibration energy from a primary system, engaging in transient resonance with a set of most energetic modes. Targeted energy transfers were utilized for suppressing regenerative instabilities in a single-degree-of-freedom (SDOF) machine tool model by coupling an ungrounded nonlinear energy sink (NES) in [11].

In this work we extend the previous study on TETs for chatter suppression in an SDOF tool model to those in a 2-DOF machining process. To properly understand the suppression mechanisms that appear similar to those in the previous aeroelastic applications [9], numerical bifurcation analysis are performed by utilizing DDEBIFTOOL [12]. The complexification-averaging technique is utilized to explore analytical TET mechanisms, which is extended to study domains of attraction by means of the asymptotic analysis.

## SYSTEM DESCRIPTIONS

We consider the dynamics of the 2-DOF machine tool model depicted in Fig. 1. Following the derivations summarized in [13], we can write down the equations of motion

$$m\ddot{x} + c_x\dot{x} + k_x x = F_x, \quad m\ddot{y} + c_y\dot{y} + k_y y = F_y \tag{1}$$

where the forcing terms can be expressed as

$$F_x = -F_C \sin\eta + F_T \cos\eta, \quad F_y = -F_C \cos\eta - F_T \sin\eta \tag{2}$$

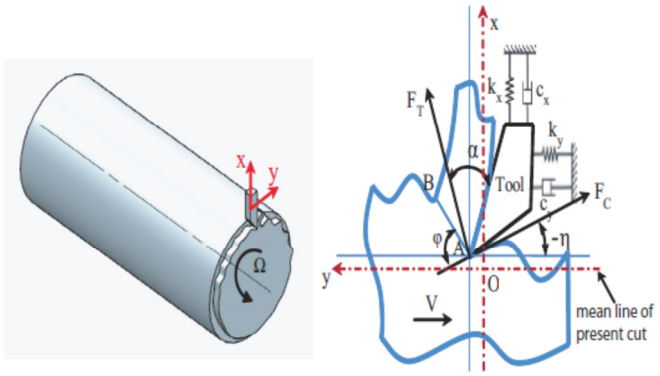


**FIGURE 1. 2-DOF MACHINE TOOL MODEL [13]**

And, $\eta$ is the angle between the x axis and the normal to the wavy surface (Fig. 1) so that $\eta = \tan^{-1}\left(\dot{x}/(V+\dot{y})\right)$. $F_T$ and $F_C$ are the thrust and cutting forces, respectively, and they can be expressed as

$$F_T = w\tau\left(s_0 - x + x_\tau\right)\frac{\sin\left(K-2\phi\right)}{\sin\phi\cos\left(K-\phi\right)}$$
$$F_C = w\tau\left(s_0 - x + x_\tau\right)\frac{\cos\left(K-2\phi\right)}{\sin\phi\cos\left(K-\phi\right)} \quad (3)$$

where, $w$ and $s_0$ are chip width and nominal chip thickness respectively. Moreover, $\tau_s$ is the shear stress in a plane called shear plane along AB line in Fig. 1. The regenerative effect of the machine tool is presented in $x_\tau = x(t-\tau)$. For any given workpiece and tool materials, an empirical relation between the shear angle $\phi$ and the friction angle $\lambda$ through experimentation can be established as $2\phi + \lambda - \alpha = K$ where $K$ is a constant depending on the cutting condition of the continuous chip formation process and $\alpha$ is rake angle.

Assuming small motions and performing nondimensionalization [13], the equations of motion in (1) can be simply written as

$$\ddot{x} + 2\varsigma_x\dot{x} + x = p\left\{p_0\left(-x+x_\tau\right) + \left(1-x+x_\tau\right)C_x\right\}$$
$$\ddot{y} + 2\varsigma_y\varpi\dot{y} + \varpi^2 y = p\left\{R_0\left(-x+x_\tau\right) + \left(1-x+x_\tau\right)C_y\right\} \quad (4)$$

where $\varpi = \omega_y/\omega_x$ is the frequency ratio, and

$$C_x = p_{1x}\frac{\omega_x s_0\dot{x}}{V} + p_{1y}\frac{\omega_x s_0\dot{y}}{V} + p_{2x}\left(\frac{\omega_x s_0\dot{x}}{V}\right)^2 + p_{2y}\left(\frac{\omega_x s_0\dot{y}}{V}\right)^2 + p_{xy}\left(\frac{\omega_x s_0}{V}\right)^2\dot{y}\dot{x}$$
$$C_y = R_{1x}\frac{\omega_x s_0\dot{x}}{V} + R_{1y}\frac{\omega_x s_0\dot{y}}{V} + R_{2x}\left(\frac{\omega_x s_0\dot{x}}{V}\right)^2 + R_{2y}\left(\frac{\omega_x s_0\dot{y}}{V}\right)^2 + R_{xy}\left(\frac{\omega_x s_0}{V}\right)^2\dot{y}\dot{x} \quad (5)$$

In this study we adopt the system parameters from [13] as

$$p_0 = 16.879,\ p_{1x} = 54.110,\ p_{2x} = 500.28,\ R_0 = -9.514,$$
$$R_{1x} = -36.984,\ R_{2_x} = -216.06,\ p_{1y} = -9.1725,\ p_{2y} = 7.674,$$
$$p_{xy} = -117.06,\ R_{1y} = 2.8983,\ R_{2y} = -2.219,\ R_{xy} = 64.109$$

The linearized stability analysis can be performed by solving the eigenvalue problem in the following.

$$\dot{\mathbf{x}} = \mathbf{L}\mathbf{x} + \mathbf{R}\mathbf{x}_\tau + \mathbf{f}(\mathbf{x}, \mathbf{x}_\tau) \quad (6)$$

where $\mathbf{f}$ represents nonlinear part of the equations; $\mathbf{x} = \left[x, y, \dot{x}, \dot{y}\right]^T$; and

$$\mathbf{L} = \begin{bmatrix} 0 & 0 & 1 & 0 \\ 0 & 0 & 0 & 1 \\ -1 - pp_0 & 0 & -2\varsigma_x + pp_{1x}\frac{s_0\omega_x}{V} & pp_{1y}\frac{s_0\omega_x}{V} \\ -PR_0 & -\frac{\omega_y{}^2}{\omega_x{}^2} & pR_{1x}\frac{s_0\omega_x}{V} & -2\varsigma_y\frac{\omega_y}{\omega_x} + pR_{1y}\frac{s_0\omega_x}{V} \end{bmatrix}$$

$$\mathbf{R} = \begin{bmatrix} 0 & 0 & 0 & 0 \\ 0 & 0 & 0 & 0 \\ pp_0 & 0 & 0 & 0 \\ pR_0 & 0 & 0 & 0 \end{bmatrix}$$

Assuming and substituting the solution of Eq. (6) to be $\mathbf{x}(t) = \exp(\lambda t)\mathbf{X}$, then we obtain the eigenvalue problem typical for a delay-differential system.

$$\left(\lambda\mathbf{I} - \mathbf{L} - \mathbf{R}e^{-\lambda\tau}\right)\mathbf{X} = \mathbf{0} \quad (7)$$

where $\mathbf{I}$ is an identity matrix. For a nontrivial solution $\mathbf{X}$, we derive the characteristic equation as $\det\left(\lambda\mathbf{I} - \mathbf{L} - \mathbf{R}e^{-\lambda\tau}\right) = 0$.

We substitute $\lambda = j\omega$, $j^2 = -1$ into the derived characteristic equation (7) and separate the results into the real and imaginary parts, respectively. Solving these two equations simultaneously for $p$ and $\Omega$ as functions of $\omega$, we obtain the stability chart depicted in Fig. 2, which looks similar to that for an SDOF tool model in [3].

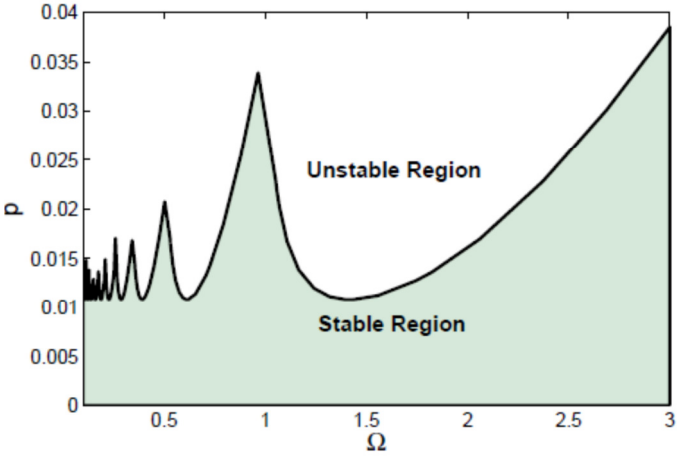


**FIGURE 2. STABILITY BOUNDARY FOR THE SYSTEM (4)**

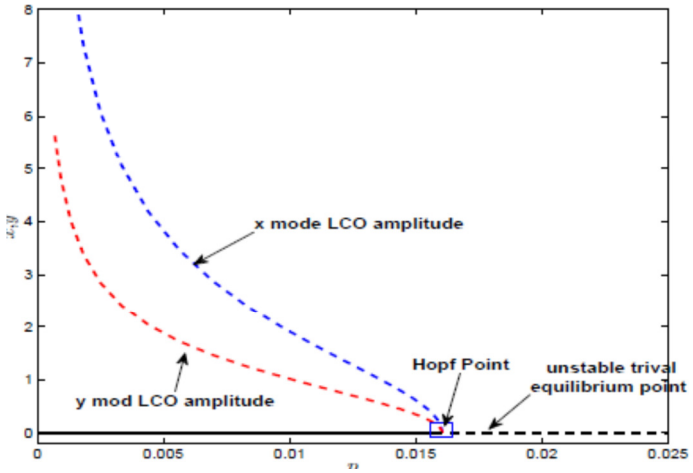


**FIGURE 3. BIFURCATION DIAGRAM FOR THE SYSTEM (4) FOR $\Omega = 2$**

In order to understand the LCOs behaviors generated at the stability boundary in Fig. 2 through a Hopf bifurcation, a numerical continuation technique is utilized (called DDEBIFTOOL [12]). For example, Fig. 3 depicts the bifurcation diagram for the trivial equilibrium and the LCOs that occur in the 2-DOF machine tool model (4) when the rotational speed of the workpiece $\Omega = 2$. It turns out that the LCO is generated through a subcritical Hopf bifurcation in this simplified model with the x-mode being more dominant. This x-mode indeed is equivalent to the mode in the previous SDOF tool model.

## APPLICATION OF NES TO X-MODE

Since we learned in the previous section that the x-mode is predominant, the NES is applied to target any energy flow fed into the x-mode, eventually eliminating the whole regenerative instability in the 2-DOF tool model (cf. Fig. 4).

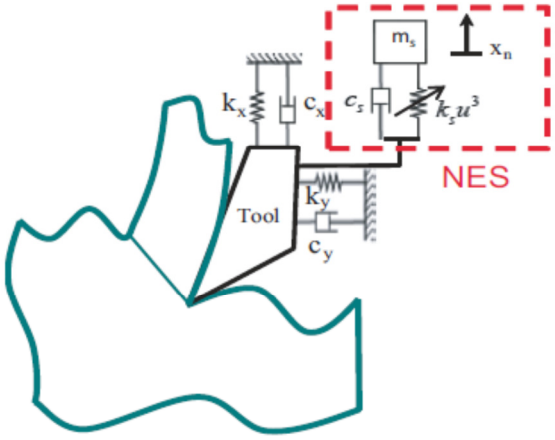


**FIGURE 4. APPLICATION OF NES TO THE X-MODE**

Then, the nondimensional equations of motion can be obtained as

$$\begin{aligned} &\ddot{x} + 2\varsigma_x \dot{x} + x + 2\varsigma_n (\dot{x} - \dot{x}_n) + C(x - x_n)^3 = F_x' \\ &\ddot{y} + 2\varsigma_y \varpi \dot{y} + \varpi^2 y = F_y' \\ &\varepsilon \ddot{x}_n + 2\varsigma_n (\dot{x}_n - \dot{x}) + C(x_n - x)^3 = 0 \end{aligned} \tag{8}$$

where $x_n$ denotes the NES displacement occurring in parallel to the x-mode; and the forcing terms can be expressed as

$$\begin{aligned} F_x' &= pp_0(-x + x_\tau) + p(1 - x + x_\tau)C_x \\ F_y' &= pR_0(-x + x_\tau) + p(1 - x + x_\tau)C_y \end{aligned} \tag{9}$$

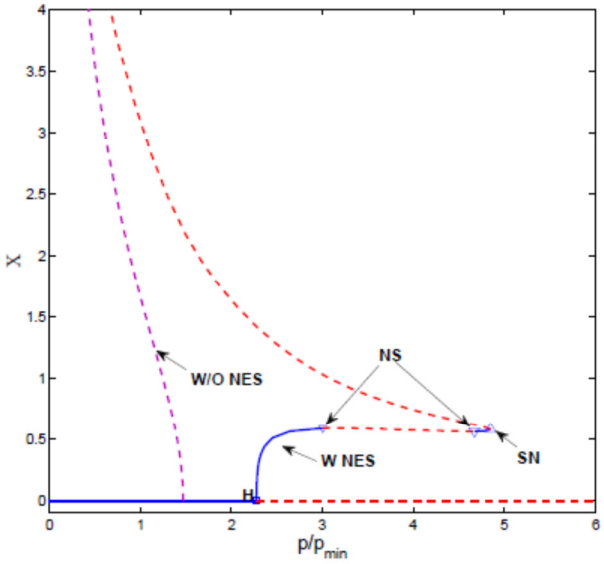


**FIGURE 5. BIFURCATION DIAGRAM WITH AN NES**

Now, as a counterpart to the bifurcation analysis in Fig. 3, we performed a numerical continuation with the NES parameters, $\grave{o} = .3, C = 0.3, \zeta_n = 0.1$, and $p_{min} = 0.0109$. The corresponding bifurcation diagram is depicted in Fig. 5. The first thing one can notice is that the types of Hopf bifurcation changes by the application of the NES to the x-mode; that is, from subcritical to supercritical Hopf bifurcations. This implies that the LCOs generated at the Hopf point with the use of an NES are stable, unlike those from the original machine tool model without the NES. Furthermore, the occurrence of the Hopf bifurcation is delayed to a higher cutting depth. However, such impressive suppression behaviors cannot be observed when the NES is coupled to the y-mode only. As depicted in Fig. 6, the subcritical Hopf bifurcation is still maintained and there is insignificant delay of Hopf point.

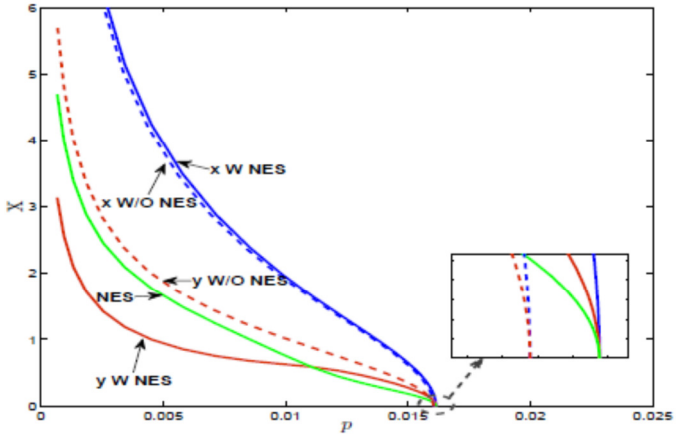


**FIGURE 6. BIFURCATION DIAGRAM WHEN THE NES IS APPLIED TO THE Y-MODE**

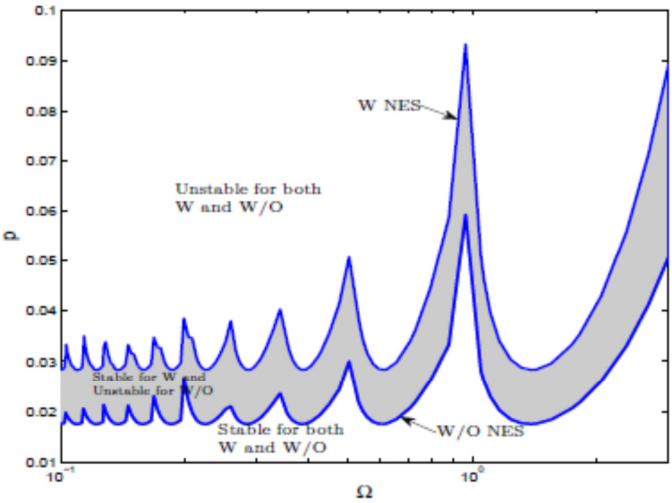


**FIGURE 7. STABILITY CHART FOR THE 2-DOF TOOL MODEL WITH AND WITHOUT NES APPLIED TO X-MODE**

Finally, Fig. 7 depicts upward shift of the stability boundary when the NES is engaged directly into the x-mode, which can be expected from the numerical bifurcation analysis in Fig. 5 illustrating that Hopf bifurcation occurs at higher cutting depth values.

As for the TET mechanisms for suppressing regenerative instabilities in this 2-DOF machine tool model, there are three distinct ones which are typically observed in many NES applications. Those mechanisms include partial ($2^{nd}$) and complete ($3^{rd}$) elimination, and recurrent burstouts and suppressions ($1^{st}$) of tool chatter. The TET phenomena involve nonlinear modal interactions between the tool modes and the NES, and Fig. 8 depicts the time series and its wavelet transform spectra for the first and third TET mechanisms.

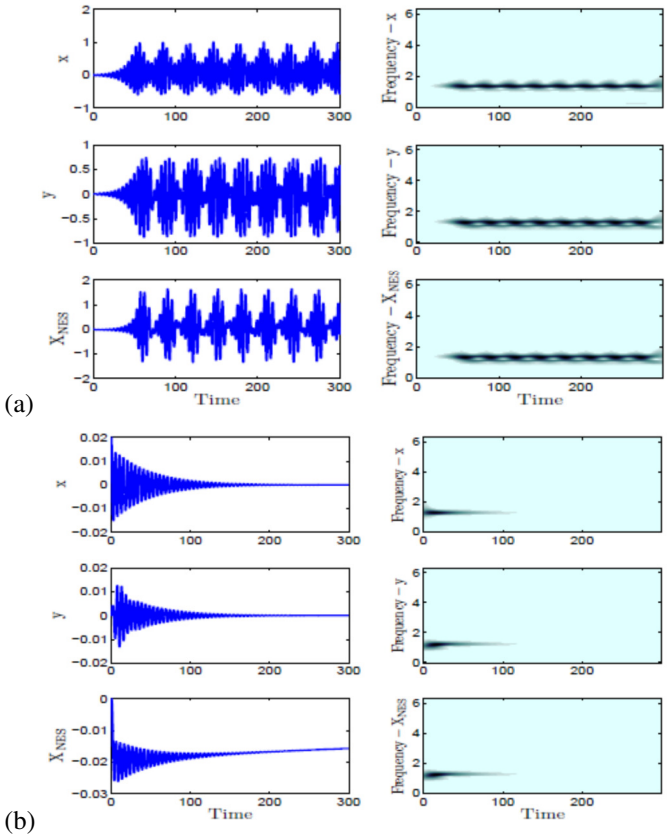


**FIGURE 8. TIME SERIES AND ITS WAVELET TRANSFORM SPECTRA FOR (a) $1^{st}$ AND (b) $3^{rd}$ TET MECHANISMS.**

## CONCLUDING REMARKS

We studied targeted energy transfer (TET) mechanisms by applying a nonlinear energy sink (NES) to suppress regenerative instabilities in a 2-DOF planar machine tool model. With the help of a numerical continuation tool, DDEBIFTOOL, we demonstrated that the tool instability is generated through a subcritical Hopf bifurcation in this simplified tool model. Studying modal energy exchanges reveals that only one of the DOFs (i.e., x-mode) is predominant, which may lead to the standard single-DOF machine tool model. Then, we applied an ungrounded NES to the 2-DOF tool model such that the NES interacts only with the dominant mode (x-mode), which turns out to be more efficient than applying the NES to the other insignificant mode (y-mode). Simple numerical simulations and bifurcation analysis demonstrated that the three typical TET mechanisms can be identified - That is, recurrent burstouts and suppression, and partial and complete suppression of tool instability.

## ACKNOWLEDGMENTS

This work was supported in part by the National Science Foundation under Grant Number CMMI-0928062.

## REFERENCES

[1] Dombovari, Z., Barton, D. A. W., Wilson, R. E., and Stepan, G., 2011. “On the Global Dynamics of Chatter inthe

orthogonal Cutting Model," *International Journal of Non-Linear Mechanics* 46, pp. 330–338.

[2] Nayfeh, A. H. and Nayfeh, N. A., 2011. "Analysis of the Cutting Tool on a Lathe," *Nonlinear Dynamics* 63, pp. 395–416.

[3] Kalmar-Nagy, T., Stepan, G., and Moon, F. C., 2001. "Subcritical Hopf Bifurcation in the Delay Equation Model for Machine Tool Vibrations," *Nonlinear Dynamics* 26, pp. 121–142.

[4] Kalmar-Nagy, T., 2009. "Practical Stability Limits in Turning (DETC2009/MSNDC-87645)," *ASME 2009 International Design Engineering Technical Conferences & Computers and Information in Engineering Conference, San Diego, California, August 30–September 2, 2009*.

[5] Lin, S. Y., Fang, Y. C., and Huang C. W., 2008. "Improvement Strategy for Machine Tool Vibration induced from the Movement of a Counterweight During Machining Process," *International Journal of Machine Tools & Manufacture* 48, pp. 870–877.

[6] Khasawneh, F. A., Mann, B. P., Insperger, T., and Stepan, G., 2009. "Increased Stability of Low-Speed Turning Through a Distributed Force and Continuous Delay Model," *Journal of Computational and Nonlinear Dynamics* 4, pp. 041003-1–12.

[7] Moradi, H., Bakhtiari-Nejad, F., and Movahhedy, M. R., 2008. "Tuneable Vibration Absorber Design to Suppress Vibrations: An Application in Boring Manufacturing Process," *Journal of Sound and Vibration* 318, pp. 93–108.

[8] Wang, M., 2011. "Feasibility Study of Nonlinear Tuned Mass Damper for Machining Chatter Suppression," *Journal of Sound and Vibration* 330, pp. 1917–1930.

[9] Vakakis, A. F., Gendelman, O., Bergman, L. A., McFarland, D. M., Kerschen, G., and Lee, Y. S., 2008. *Passive Nonlinear Targeted Energy Transfer in Mechanical and Structural Systems: I and II*, Springer-Verlag, Berlin and New York.

[10] Arnold, V. I. (Ed.), 1988. *Dynamical Systems III. Encyclopaedia of Mathematical Sciences*, Springer-Verlag,Berlin/New York.

[11] Nankali, A., Surampalli, H., Lee, Y.S., and Kalmar-Nagy, T., 'Suppression of Machine Tool Chatter using Nonlinear Energy Sink (DETC2011-48502),' *ASME 2011 International Design Engineering Technical Conferences (IDETC) and Computers and Information in Engineering Conference (CIE), Washington, DC, August 28–31, 2011*.

[12] Engelborghs, K., Luzyanina T., and Roose, D., 2002. "Numerical Bifurcation Analysis of Delay Differential Equations using DDE-BIFTOOL," *ACM Transactions on Mathematical Software* 28(1), pp. 1–21.

[13] Pothala, T., and Chandiramani, N. K., 2006, 'Dynamics of 2-DOF Regenerative Chatter During Turning', *Journal of Sound and Vibration*, 290: 448-464.

[14] Nankali, A., *Tool Chatter Suppression by Means of Targeted Energy Transfer*, MS Thesis, New Mexico State University, 2012.